

Investigation of Rock Slope Stability Using Drone-Based Thermal Sensor

Muhammad Latifi Mohd Yaacob¹, Abd Wahid Rasib^{1*}, Zulkepli Majid¹, Nor Hamizah Idgihat¹, Khairulnizam M. Idris¹, Ahmad Safuan A Rashid², Radzuan Sa'ari², Mushairry Mustaffar², Norbazlan Mohd Yusof³, Norisam Abd Rahaman³ and Rozilawati Dollah⁴

¹ Geospatial Imaging and Information Research Group, Program Geoinformation, Faculty of Built Environment and Surveying, University Teknologi Malaysia, Skudai, 81310, Johor.

²School of Civil Engineering, Faculty of Engineering, Universiti Teknologi Malaysia, Skudai, 81310, Johor.

³Centre of Excellence, Persada PLUS, Persimpangan Bertingkat Subang, KM 15, Lebuhraya Baru, Lembah Klang, 47301, Petaling Jaya, Selangor.

⁴School of Computing, Faculty of Engineering, Universiti Teknologi Malaysia, 81310 UTM Johor Bahru, Johor, Malaysia

*Correspondence email: abdwahid@utm.my

Abstract- This study focuses on the investigation of rock slope stability using a drone-based thermal sensor. In this study, a compact remote sensor of visible spectrum (400–700 nm) and infrared thermography spectrum (7,500–13,500 nm) was used to develop a method for monitoring the stability of rock slope failure in terms of temperature. This study used two datasets of each sensor that were collected in two different phases. The first phase was conducted during the dry season, which was completed in October 2019. Meanwhile, the second phase was carried out during the wet season in December 2019. The study area is located at a rock slope structure of KM 257.5 to KM 258.3, which is approximately 800 m in length at the North-South Expressway (PLUS). The location is situated after the Menora tunnel in Jelapang, Perak, Malaysia, facing southbound. This study is helpful in illustrating how drone-based remote sensing is implemented in rock slope investigations. The results from this study indicate that rock slope instability can be identified through the thermal image of surface temperature. Finally, this study determines that a rock slope is less stable in cooler temperatures compared to warmer temperatures. Rock slope failure tends to occur at a cooler surface, especially for wedge and toppling failure.

Keywords - Rock Slope, Temperature, Rock Failure, Drone-Based Thermal Sensor

©2022 Penerbit UTM Press. All rights reserved.

Article History: Received 21 January 2022, Accepted 25 March 2022, Published 31 March 2022

How to cite: Yaacob, M.L.M., Rasib, A.W., Majid, Z., Idgihat, N.H., Idris, K.M., Rashid, A.S.A., Sa'ari, R., Mustaffar, M., Yusof, N.M., Rahaman, N.A., Dollah, R. (2022). Investigation of Rock Slope Stability Using Drone-Based Thermal Sensor. Journal of Advanced Geospatial Science & Technology. 2(1), 67-91.

1. Introduction

The formation of rock slope instabilities is governed by structural and lithological characteristics, such as faults, folds, joints, foliation, and bedding planes that provide kinematic flexibility to potentially cause an unstable block at scales ranging from outcrops and roadcuts to the entire mountain slope [1]. The typical natural process acting on rock slopes is rockfall. According to Crosta et al. [7], the downward movement of unattached rock particles due to free-falling, bouncing, rolling, and sliding is known as rockfall. The weathering of bedrock outcrops on steep slopes, the eventual separation of the weathering products, and their removal downslope cause rockfalls. Rockfalls are rare, irregular, and unpredictable, making it impossible to compile long or reliable records of their size and frequency [20]. According to Robbins [28], rockfalls frequently occur along road corridors caused by deep cuts into rock slopes. Rockfalls are most common in rock-cut slopes when rock blocks are displaced by weather, running water, or erosion of the surrounding rocks and soil. Furthermore, rockfalls are difficult to forecast due to the uneven, unexpected character of rock joints and weathering patterns.

2. Literature Review

Rock Stability

According to Pantelidis [25], rock slopes in most road cuts, especially in mountain areas, are exposed to instability problems. These problems occur due to the variation in the rock mass conditions and external factors of the environment, such as seismic activities and water on the slope. The stability of rock slope is a crucial factor that needs to be considered for public safety because it often occurs near the area of the highway passing through rock cuts, as well as for equipment safety and personnel in open-pit mines [5].

The instability of slopes and road cuts is determined by the material characteristics of the rock slope, the face angle, the height, and the rock joint orientation. Rock slope stability is also influenced by road curvature, particularly in rugged terrains [14]. Siad et al. [32] stated that rock material and discontinuities control the failure of rock slopes. Failure surface cuts through intact rock for heavily jointed rock masses with weak rock material. Meanwhile, joint planes are mostly responsible for the failure of rock masses with fewer joints and stronger rock material.

Rock Properties

The physical properties of rocks are beneficial in many fields of work, including geology, petrophysics, geophysics, materials science, geochemistry, and geotechnical engineering. Density, porosity, and permeability are examples of rock physical properties, whereas elastic modulus, Poisson's ratio, and rock strength are examples of rock mechanical properties. The physical properties of rock-forming minerals and the type of mineral bonding are related to rock material properties. Qualitative techniques, basic classification tests, and laboratory testing are used to identify properties from hand specimens, core sections, drill cuttings, outcroppings, and disturbing materials [36].

For slopes and channels, the rate of sediment removal must be higher than the rate of sediment production or supply, which is determined by soil production, rock mass strength, rock uplift rate, river discharge/debris flow/landslide magnitude-frequency attributes, and inherited factors related to quaternary climate change [17].

Thermography Rock Slope

Ground-based technologies, such as digital photogrammetry, terrestrial laser scanning, ground-based interferometric synthetic aperture radar, and infrared thermography have been increasingly used as efficient remote surveying techniques for rapid characterisation and mapping of slopes affected by instability processes, which are among the new methods for accurate landslide mapping. The field of remote sensing known as thermal imaging deals with detecting the radiant temperature of the Earth's surface features from afar [33].

Thermal infrared sensors have been employed in environmental research in various platforms since the 1980s, including terrestrial, aerial, and spaceborne platforms. The sensors have been used in the context of mining [30]. In recent years, there have been significant advancements in drone technology and also a broad range of applications to which the technology has been deployed. Drones are used in the photogrammetric platform to obtain spatial data of an area for both local- and large-scale applications in various circumstances [8]. A low-cost photogrammetric method that uses a drone or an unmanned aerial vehicle (UAV) has been increasingly used to solve engineering-geological problems. This method is known as Structure from Motion (SfM), which is the basic principle of stereoscopic photogrammetry. In this research, thermal imaging was used with a drone for data mining, which is a process used

to turn raw data into useful information. The raw data from the thermal image were converted into a grayscale image, followed by filtering.

Rock Slope Failure

Rock slope failure has occurred every year on the Earth over the past century, and there have been two or more failures in some years. Rock slope failures larger than 1 km³ are much less frequent, and recent events of this size described in the scientific literature are only the 1911 Usoi landslide in Tajikistan [29] and the 1974 Mayunmarca landslide in Peru [18].

According to Wyllie and Mah [37], most rock slope failures can be classified into four categories depending on the type and degree of structural control shown in **Figures 1–4**. The types of rock slope failures are as follows:

- I. Planar failures are governed by a single discontinuity surface dipping out of a slope face.
- II. Wedge failures involve a failure mass defined by two discontinuities with a line of intersection that is inclined out of the slope face.
- III. Toppling failures involve slabs or columns of rock defined by discontinuities that dip steeply into the slope face.
- IV. Circular failures occur in rock masses that are either highly fractured or composed of material with low intact strength.

It is difficult to estimate the likelihood of failure. The yearly frequency of landslides of a specific size per 10,000 km² of a hilly terrain or the number of incidents per thousand years per area are examples of regional-scale failure probability measurements [16]. Such approaches are ineffective at the local level, where it may be essential to estimate the likelihood that a particular slope would collapse [13].

2. Methodology

This research aims to investigate rock slope stability using a drone-based thermal sensor. Slope stability depends on the geological and geotechnical characteristics of the bedrock and soil that compose the slopes. Thus, the strength of these materials is vital to slope stability. In this study, a drone-based thermal sensor was used to obtain the black hot image of the rock slope's surface

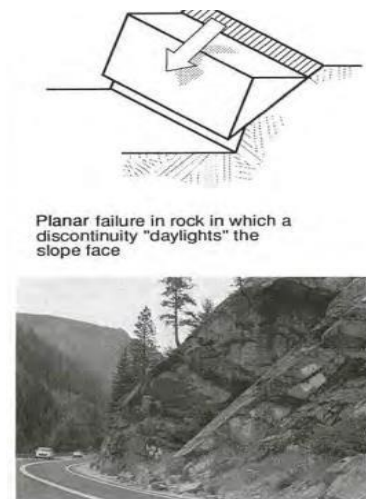


Figure 1: Planar failure in the rock, in which a discontinuity “daylight” the slope faces [37].

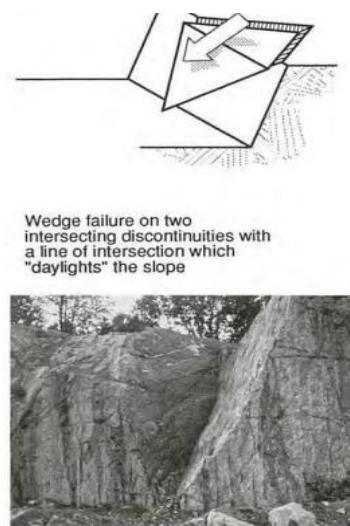


Figure 2: Wedge failure on two intersecting discontinuities with a line of intersection which “daylights” the slope [37].

temperature. The result of the segmentation can be known, in which the failure area is considered failure based on temperature, according to Al-Bared et al. [4].

The three research problems identified during this research are:

- i) The rock slope stability in terms of temperature according to rock slope failure.
- ii) Visualisation of the rock slope's surface temperature using a drone-based thermal sensor.
- iii) The interpretation between the rock slope's surface temperature and rock slope failure.

The proposed method is to use a drone-based thermal sensor to obtain the black hot image of the rock slope's surface temperature, followed by segmentation, which is a map-making method proposed to obtain the final results. The flow of this study consists of four stages: data acquisition, data processing, data analysis, and results and analysis.

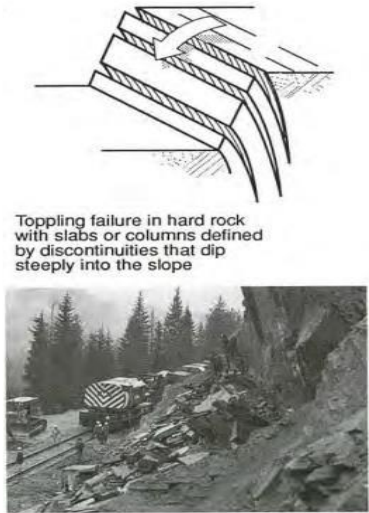


Figure 3: Toppling failure in hand rock with slabs or columns defined by continuities that dip steeply into the slope [37].

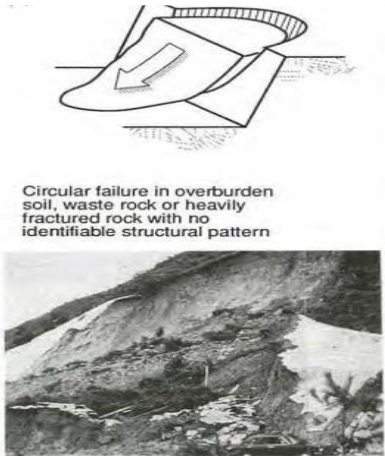


Figure 4: Circular failure in overburden soil, waste rock or heavily fractured rock with no identifiable structural pattern [37].

Research Design and Planning

The main idea of this phase is to review the literature regarding the issues and problems related to the topic, as well as setting up the data sources and overall methodology. Then, the study area, source preparation, the instrument used, and also the flight planning for the UAV data are identified. The UAV image acquisition with a thermal camera is necessary to create a digital terrain model. The UAV data was captured using a DJI Inspire 2 drone due to its ability to move above the strictly programmed trajectory and to produce pictures at equal intervals and programmed camera orientation. The thermal camera used for drone mapping has a high resolution of 640×512 pixels. This resolution can distinguish objects measuring only a few centimetres from a height of 360 m. Furthermore, the camera is also equipped with GPS; hence, each picture stores coordinates in a convenient file when starting to stitch an image.

The UAV image acquisition used nadir flight with a thermal camera. A series of nadir images for phase 1 and 2 were captured with a high degree of overlap in the horizontal and vertical directions covering the study area. The acquired images serve as the inputs to Pix4Dmapper software and generate a point cloud coordinate to further generate a digital surface model (DSM), digital orthophoto images, and 3D surface models. In total, 630 and 230 images were captured in phase 1 and 2, respectively, and these images were obtained for 3D modelling. For dense point cloud generation, the workflow consists of initial processing, point cloud densification, image grouping, point cloud filter, and 3D textured mesh setting. The images were filtered using the processing area, where this option was chosen to filter the point cloud and the 3D textured mesh. The final process is the visualisation of the thermal index map for phase 1 and 2.

Data Acquisition

The study area is located at a rock slope structure of KM 257.5 to KM 258.3, which is approximately 800 m in length. The area is situated after the Menora tunnel in Jelapang, Perak, Malaysia, facing southbound, as presented in **Figures 5 (a) and (b)**. This study used two datasets of each sensor collected in a different phase. Phase 1 was carried out during the dry season, which was completed in October 2019. During phase 1 of data collection, the weather was a little hazy with a temperature of 33 °C. Meanwhile, phase 2 was conducted during the

wet season in December 2019. During phase 2 of data collection, the weather was clear with a temperature of 32 °C even though it was carried out during the wet season.



Figure 5: (a) The study Area of the Menora tunnel in Jelapang, Perak, Malaysia and (b) a street view by Google Maps, 2018.

A FLIR Zenmuse XT camera (**Figure 6 (a)**) attached to the drone DJI Inspire 2 (**Figure 6 (b)**) was used in this stage. The details of the sensor of the FLIR Zenmuse XT thermal camera and the drone are shown in **Tables 1 and 2**.

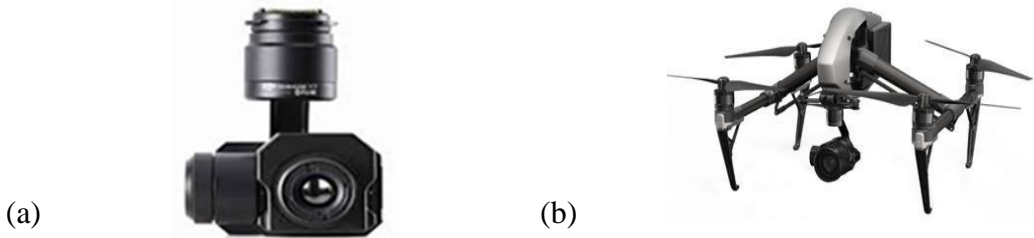


Figure 6: (a) FLIR Zenmuse XT and (b), DJI Inspire 2 drone (Photo By DJI Company, 2019).

Table 1: Specification of DJI FLIR Vue Pro thermal camera, FLIR Zenmuse XT.

Instrument	Specification
FLIR Zenmuse XT	Lens: 13 mm lens Resolution: 640 × 512 pixels Spatial Resolution: 0.4 cm Spectral Range: 7.5–13.5 μm Thermal Imager: Uncooled VOx microbolometer

Table 2: Specification of the drone, DJI Inspire 2.

Instrument	Specification
DJI Inspire 2	Payload: 3.2 kg Flight Autonomous: 27 min Velocity Range: 10 m/s at height of 2 m Altitude Range: 10 m Operating Range: 10 m Obstacle Sensing Range: 0.7–30 m

Data Processing

Upon completion of data acquisition, the subsequent phase is data processing. Raw data were converted into a grayscale image, followed by filtering. This study used an edge detection filtering method. Using the concept of gradient detection, this approach was used to categorise the form of objects in thermal imaging. The gradient is the brightness difference in the imagery that is specified spatially. The gradient reaches the maximum value in areas where the brightness of neighbouring pixels varies the most. Subsequently, the image was resized to eliminate the unwanted part of the rock slope image. The data from the thermal image were converted from the grayscale data format to the surface temperature using FLIR Tools Software. After that, the image was subjected to mosaicking to create an orthophoto image using Pix4Dmapper Software. The observation was done for the orthophoto image to determine the potential area where rock slope instability could occur.

Output and Analysis

Data analysis was conducted by emphasising the qualitative method based on only visual analysis. The analysis was used for a faster and more intuitive interpretation of the rock slope condition using the thermal image and temperature reading. The image was analysed in two steps. First, the image was visualised for surface mapping. Second, the surface temperature range of the rock slope was interpreted to detect the unstable rock slope based on the temperature range. Subsequently, the segmentation was performed based on several surface temperature areas to evaluate rock stability.

Visualisation of Surface Temperature Mapping

Figure 7 (a) presents the surface mapping of phase 1 generated by Pix4Dmapper Software. In this mapping, five spot areas of segmentation were randomly selected. Each segmentation illustrates a different spot in the study area. **Figure 7 (b)** shows the surface mapping of phase 2 generated by Pix4Dmapper Software. **Figures 8 (a) and 8 (b) to 12 (a) and 12 (b)** illustrate one of the several images in the segmentation area from Sp1 to Sp5, respectively. Meanwhile, for phase 2, the segmentation of phase 1 was randomly selected.

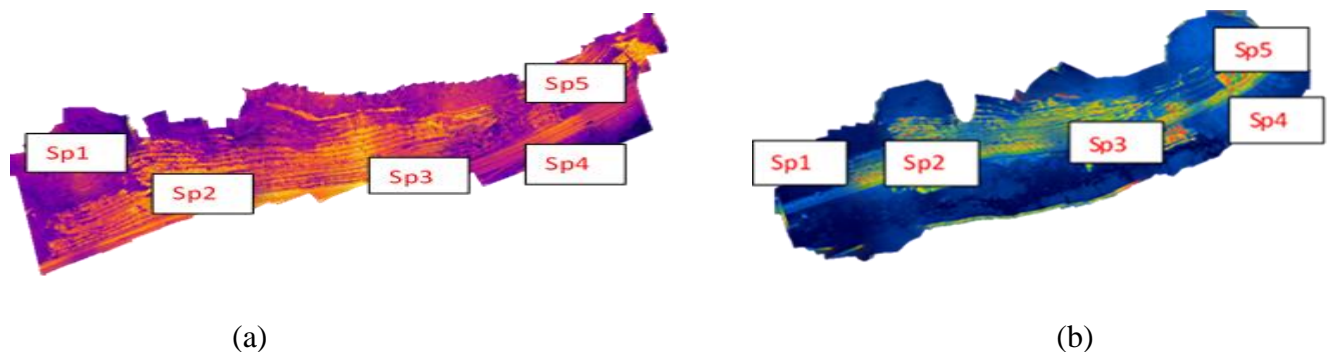
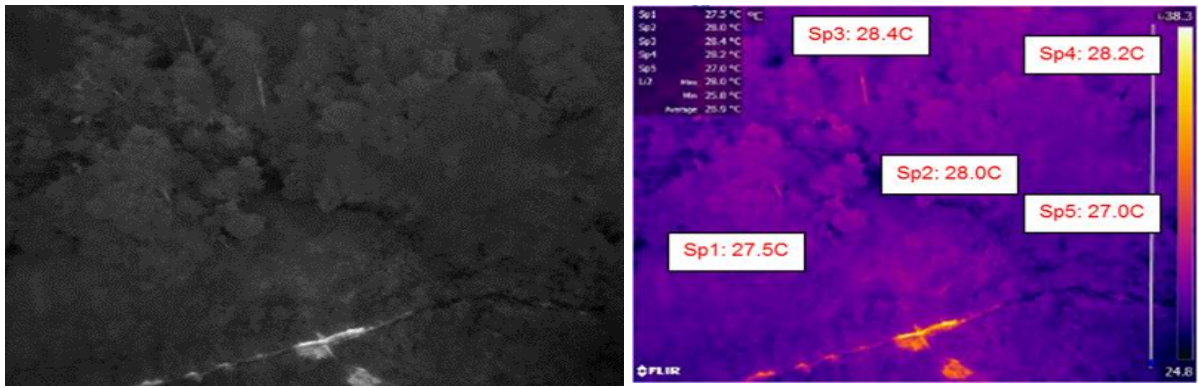


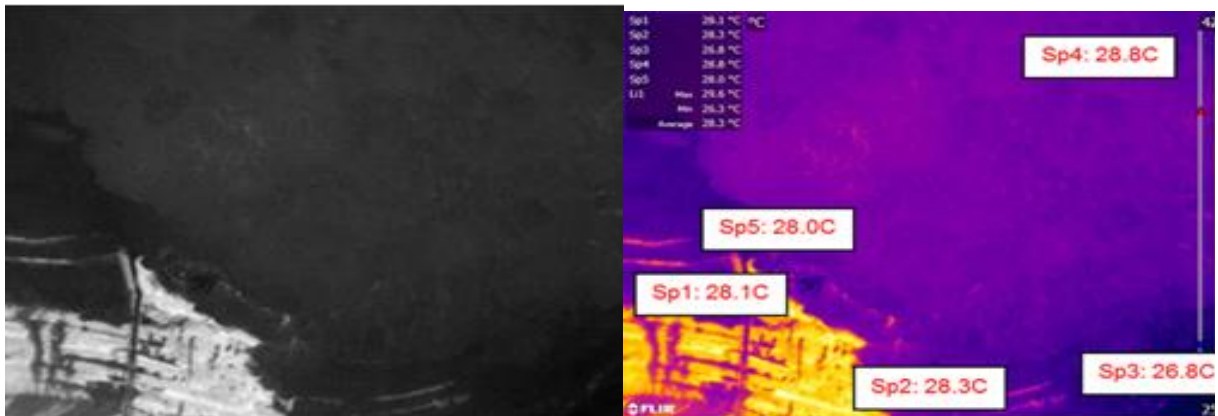
Figure 7: Surface mapping of (a) phase 1 and (b) phase 2 generated by Pix4Dmapper software.

Figures 8 (c) and 8 (d) to 12 (c) and 12 (d) illustrate one of the several images in the segmentation area from Sp1 to Sp5, respectively. Sp1 is a vegetation area, Sp2 is a rock slope area, Sp3 is a roadway area, Sp4 is the ravine beside a roadway area, and Sp5 is another rock slope area. The map shows that different surfaces of the thermal image have different temperatures. The different temperatures are based on the density colour of the map surfaces. Lighter or brighter areas indicate warmer areas, while darker areas represent cooler areas.



(a)

(b)



(c)

(d)

Figure 8: (a) The original image of Sp1 in phase 1 from a drone-based thermal sensor, (b) the thermal photo from FLIRR software in phase 1, (c) the black hot image of Sp1 in phase 2 from a drone-based thermal sensor, and (d) the thermal photo from FLIRR software in phase 2 (Sp1 is a vegetation area).

Rock Slope Failure Determination from Surface Temperature

In this study, the potential occurrence of four types of rock slope failure surface was identified based on the image interpretation of the rock slope failure characteristics. The potential of rock slope failure occurrence was marked in a red circle. The temperature reading was simultaneously spotted in five areas. **Figures 13 (a) and 13 (b) to 16 (a) and 16 (b)** show the temperature reading at the exact location for each type of rock slope failure in phase 1 and 2, respectively.

Planar rock slope failure generally occurs when a structural discontinuity plane dips or daylight towards the valley at an angle smaller than the slope face angle and greater than the angle of friction of the discontinuity surface [34] [19]. The red circle in **Figures 13 (a) and 13 (b)** show the characteristics with the potential of planar failure, which is the dip of the planar discontinuity less than the dip of the slope face and facing daylight at the slope face. In addition, according to Raguvanshi [27], the tension crack must be present in the upper portion of the slope, which can be seen from the black oval in **Figures 13 (a) and 13 (b)**. Tension crack can occur at the surface with the highest surface [9].

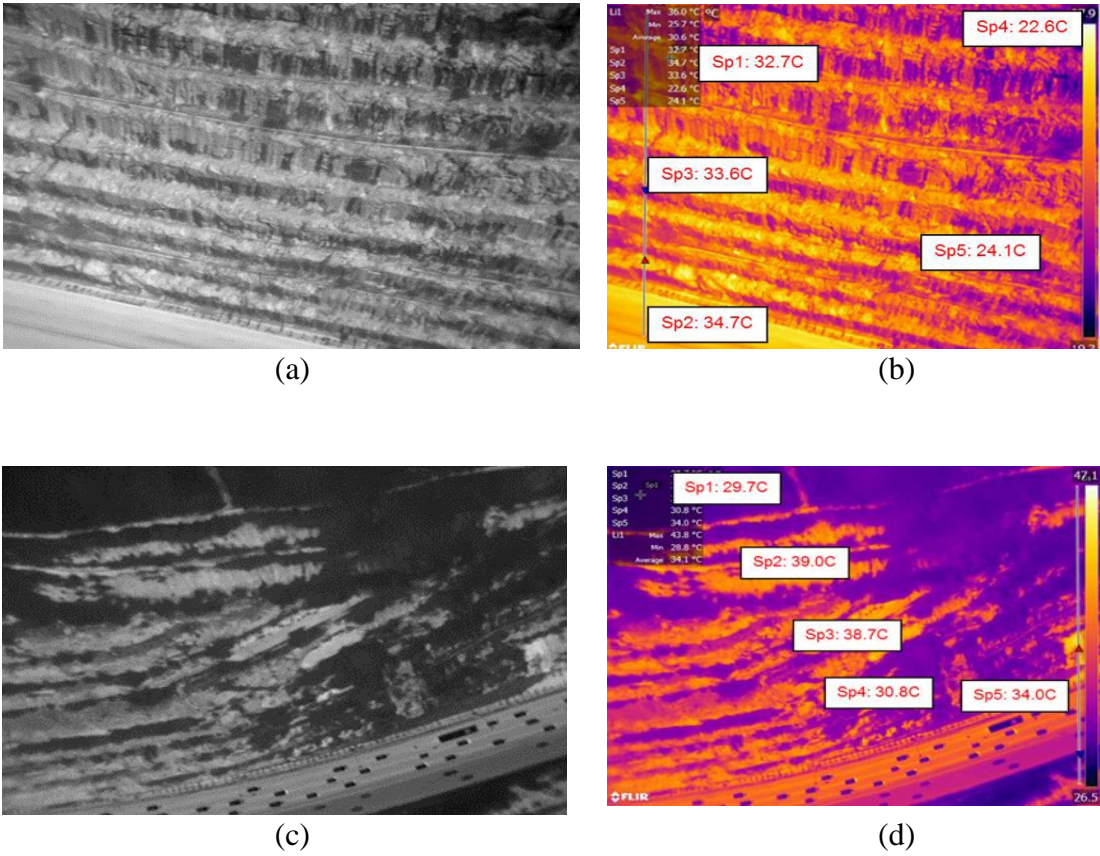


Figure 9: (a) The black hot image of Sp2 in phase 1 from a drone-based thermal sensor, (b) the thermal photo from FLIRR software in phase 1, (c) the black hot image of Sp2 in phase 2 from a drone-based thermal sensor, and (d) the thermal photo from FLIRR software in phase 2 (Sp2 is a rock slope area).

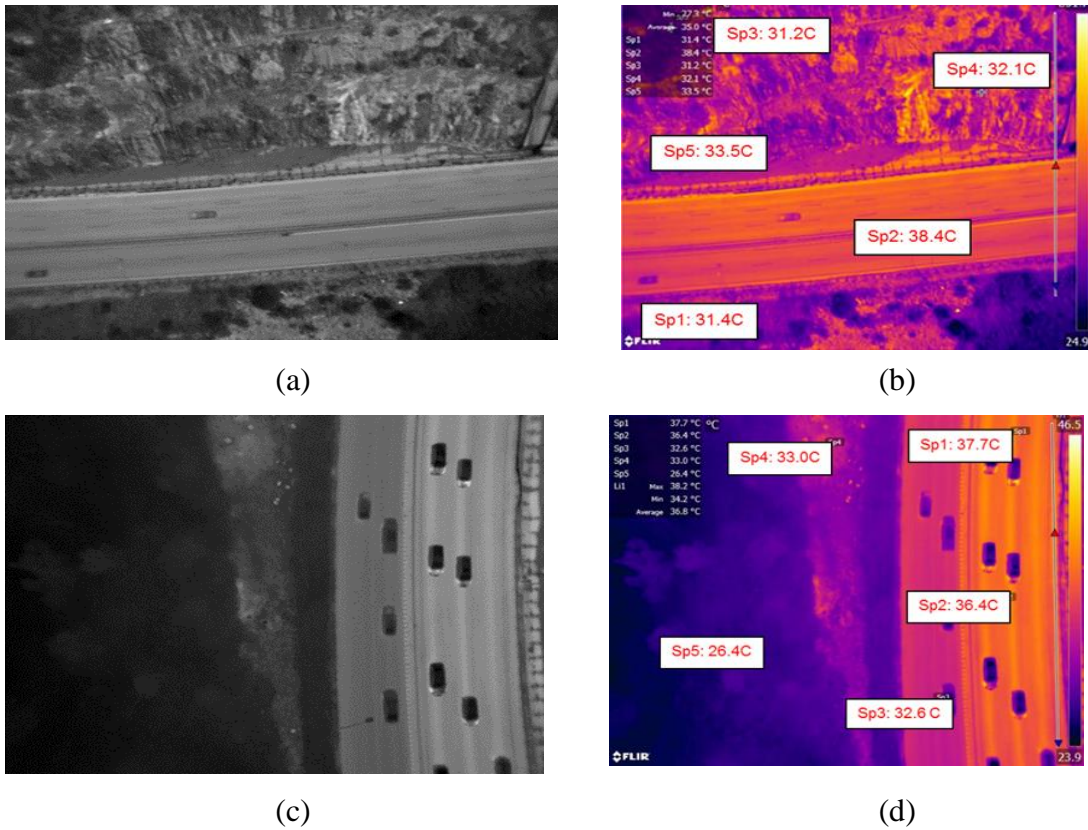
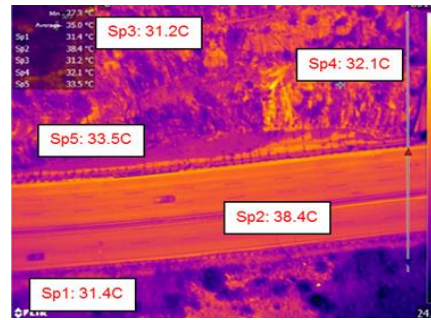


Figure 10 (a) The black hot image of Sp3 in phase 1 from a drone-based thermal sensor, (b) the thermal photo from FLIRR software in phase 1, (c) the black hot image of Sp3 in phase 2 from a drone-based thermal sensor, and (d) the thermal photo from FLIRR software in phase 2 (Sp3 is a road way area).

Wedge failure is predicted when the rock mass slides along two intersecting discontinuities, both of which dip out of the cut slope at an oblique angle to the cut face. The wedge initial development is defined by the intersecting planes of fractures, cleavage, bedding, or all three features, resulting in the formation of V-shape wedges of unstable rock, as shown in **Figures 14 (a) and 14 (b)**. The size of wedge failure can range from a few cubic meters to a very large slide. A typical rock cut along a highway in which geological structure is conducive to wedge failure results in an unstable slope condition [24].



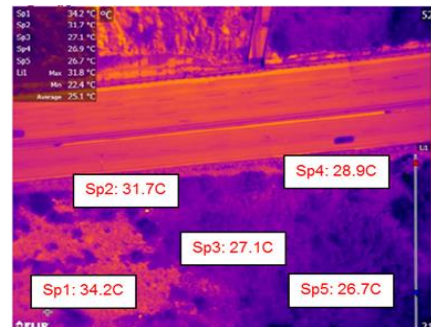
(a)



(b)



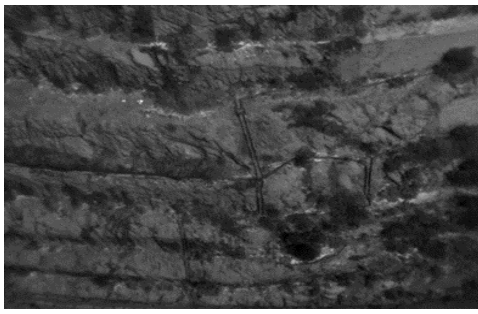
(c)



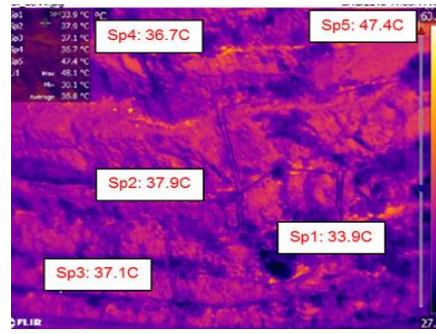
(d)

Figure 11: (a) The black hot image of Sp4 in phase 1 from a drone-based thermal sensor, (b) the thermal photo from FLIRR software in phase 1, (c) the black hot image of Sp4 in phase 2 from a drone-based thermal sensor, and (d) the thermal photo from FLIRR software in phase 2 (Sp4 is a ravine beside the roadway area).

Block toppling occurs in hard rock when individual blocks or columns are formed of two normal joint sets, with the main set dipping steeply into the face, as shown in the red circle in **Figures 15 (a) and 15 (b)**. The upper blocks tend to topple and push forward on the short columns in the slope toe [3]. Toppling failure is typical for rock masses that have been broken into a series of slabs or columns by a set of fractures that run roughly parallel to the slope face and deep into the face. Toppling failure occurs when a rock column or slab rotates about an essentially fixed point at or near the slope's base while slippage occurs between two layers. Toppling failure is characterised by a horizontal movement at the crest and minimal movement at the toe [24].



(a)



(b)



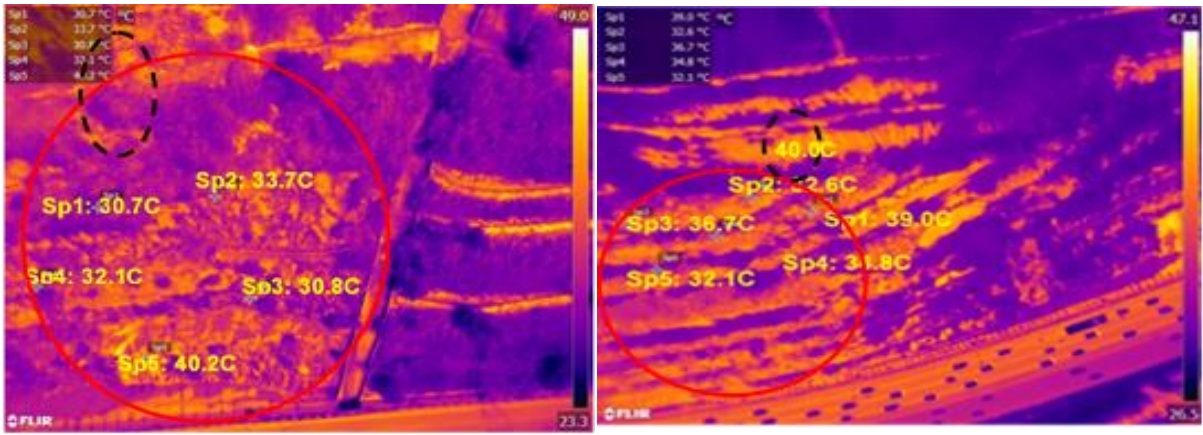
(c)



(d)

Figure 12: (a) The black hot image of Sp5 in phase 1 from a drone-based thermal sensor, (b) the thermal photo from FLIR software in phase 1, (c) the black hot image of Sp5 in phase 2 from a drone-based thermal sensor, and (d) the thermal photo from FLIR software in phase 2 (Sp5 is a rock slope area).

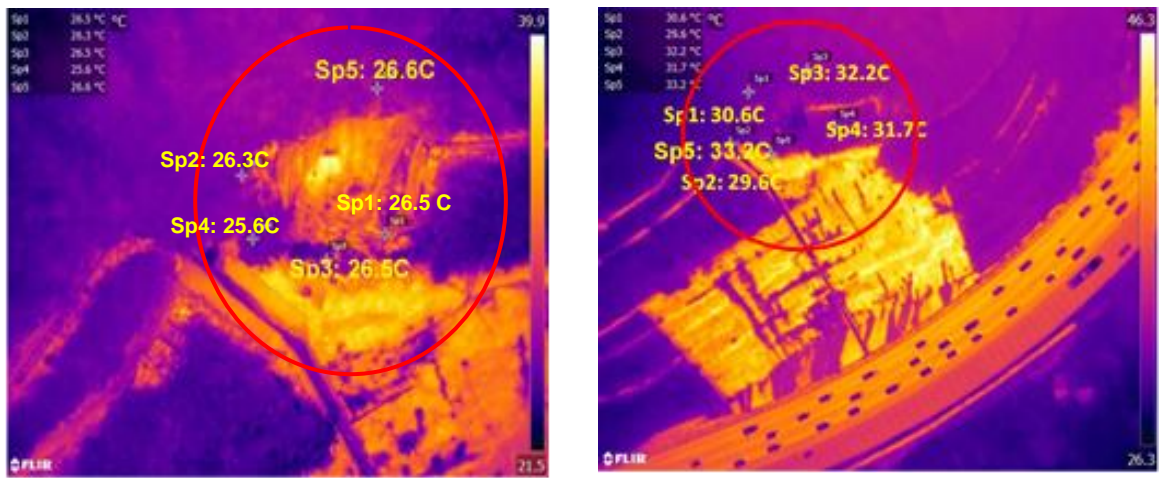
The characteristics of circular failure in rock are similar to those of classical rotational loss in soil, except that the failure surface in the rock tends to form a shallow, large-radius circle, as shown in the red circle in **Figures 16 (a) and 16 (b)**. The sign of slope distress precedes the rotational failure in rock. These distress signs include precise tension crack near the crest of the slope that bulges into the toe area of the slide and longitudinal cracks parallel to the inclination of the slope face. The types of rock susceptible to circular failure include those that are close and randomly fractured [24].



(a)

(b)

Figure 13: Planar failure temperature of (a) phase 1 and (b) phase 2 in the study area.



(a)

(b)

Figure 14: Wedge failure temperature of (a) phase 1 and (b) phase 2 in the study area.

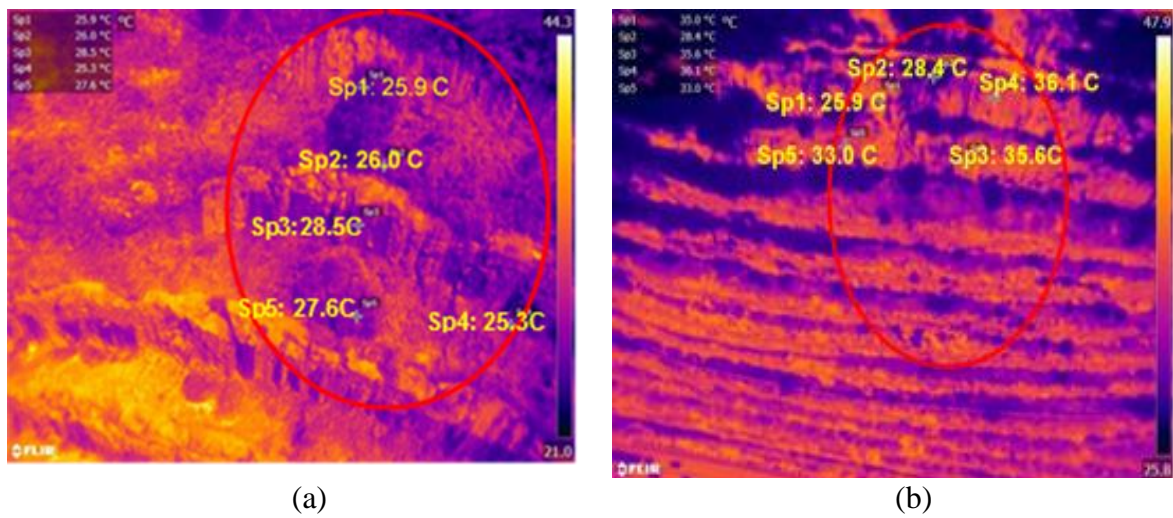


Figure 15: Toppling failure temperature of (a) phase 1 and (b) phase 2 in the study area.

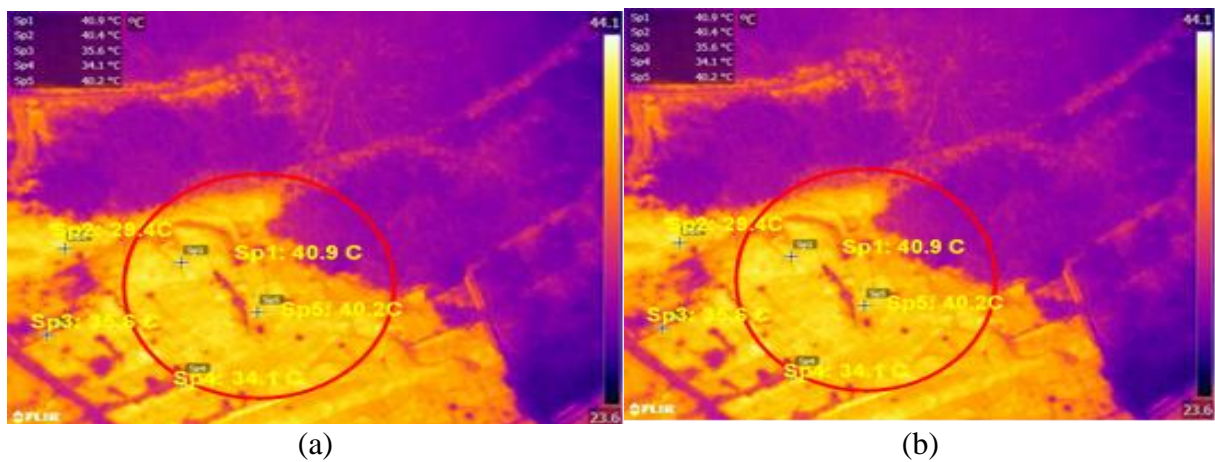


Figure 16: Circular failure temperature of (a) phase 1 and (b) phase 2 in the study area.

3. Results and Discussion

The results show that most rock slope instability in the geological conditions of rock surfaces are related to the current temperature. Based on the investigation of the rock slope, the instability condition can be identified by various factors involving human interaction and the physical environment. According to Al-Bared [4], degradation is one of the factors in slope instability. Weathering elements, such as water, wind, temperature, and ice deteriorate the

slope's strength and the slope-forming materials. Weathering is important in reducing the stability of rock slopes by forming unfavourable orientations that deteriorate strength [15].

Figures 13 (a) and 13 (b) to 16 (a) and 16 (b) show the image pairs for phase 1 and 2 based on the temperature for different types of rock slope failure. For planar rock slope failure, the surface temperature of phase 1 ranges between 30.7 °C and 40.2 °C in the dry season. Meanwhile, the temperature range of phase 2 is from 32.1 °C to 39.0 °C during the wet season. For wedge rock slope failure, the temperature range of phase 1 is between 26.3 °C and 26.6 °C and between 29.6 °C and 32.2 °C for phase 2 . The temperature ranges of toppling rock slope failure in phase 1 and 2 are from 25.3 °C to 28.5 °C and from 25.9 °C to 35.6 °C, respectively. Finally, the temperature range of circular rock slope failure in phase 1 is between 29.4 °C and 40.9 °C and between 37.4 °C to 43.8 °C for phase 2. This result shows that thermal anomaly is related to slope instabilities in terms of rock slope failure. The surface temperature is represented by different means of colour scale. Warmer and cooler temperatures are displayed by lighter and darker colours, respectively. Thus, the surface temperature between 25.9 °C and 28.5 °C is under cooler temperature anomalies, while the surface temperature between 28.6 °C and 43.8 °C is considered warm temperatures.

Wedge and toppling failure could occur in phase 1. The temperature range detected for planar and circular failure did not differ significantly in phase 1 and 2. Hence the probability of occurrence of planar and circular failure is similar for both phases. Although the temperature range for phase 2 is higher than phase 1, it does not mean that rock slope failure will not occur in phase 2. Many factors influence rock slope failure other than surface temperature. According to Ulusay [35], four main factors including lithology (rock type), structure (discontinuities), state of degradation, and hydrogeological conditions prevailing in rock slopes can lead to slope failure. The instability in slopes primarily depends on the relationship between driving and resisting forces and the slope height increased the slope susceptibility for instability [14].

The presence of multiband colour composites due to multiple wavelengths of thermal emission is recorded; thus, the potential of rock slope failure increased with a cooler surface temperature. The deformation and failure of rock slope will result in the occurrence of landslides step by step. Temperature increases the contact surface between particles, which is dependent on the coefficient of thermal expansion of mineral components. This causes structural changes, which affect the values of strength parameters and the rock's bulk density [26]; [21]; [39]. According to Shibasaki [30], many reactivation-type landslides become active during cold seasons, and some landslide begins to move during the early cold season.

According to Guerin et al. [10], cooler temperature represents the loose rock section. Temperature is an essential part of rock creation, modification, and destruction. Meanwhile, weathering is the first step in the breakdown of rock into smaller fragments. Rocks expand when they heat up in the sun and contract as they cool down at night. Different minerals expand and contract at different rates in response to heating and cooling, causing stresses along mineral boundaries. Thus, rock slope instability in this study is expected to be affected by the cooler temperature. It can be seen from the temperature range for each spot area of the five images used. The temperature reading for the Sp1 area in both phase 1 and 2 between 26.8 °C and 28.8 °C is lower than in other spot areas.

The Sp1 area for both phase 1 and 2 represents the vegetation area. The potential of plants growing on slopes to support and inhibit slope stability is linked to vegetation and slope stability. The relationship is a complex combination of the type of soil, the rainfall regime, the plant species present, the slope aspect, and the steepness of the slope [22]. Steep vegetated slopes are stabilised by vegetation, which reinforces the soil through tree roots and changes the soil water regime. Seasonally, pore water pressures in the soil fluctuate in response to precipitation. Soil moisture is frequently higher in regions where the forest has recently been cut than in uncut areas.

Increased apparent soil cohesiveness has been interpreted as root reinforcement. The finite element method was used to incorporate the apparent root cohesion into the slope stability study [23]. According to Akinola et al. [2], a cohesive soil erosion rate in rock slope decreased with increased soil temperature and increased as eroding water temperature increased. Thus, in this study, the degradation of rock slope surface is influenced by the soil and water temperature.

Apart from vegetation, rainfall also results in a cooler temperature. The failure mechanism for rainfall-induced shallow failures is that as water infiltrates into the soil, the soil matric suction decreases and the pore pressure increases. The change in water content after rainfall infiltrates into the soil generates an increase in suction stress (a decrease in its absolute value). Slope instability occurs as a result of the reduced soil effective stress [38].

The results of phase 1 of this study have shown that high-temperature surface coverage is more than cooler temperature. It can be seen in Figure 7 (a) that there are more “iron” brighter coloured areas than the darker coloured areas. This is because the data in phase 1 were collected in the dry season in October 2019. Meanwhile, the surface mapping of phase 2 in Figure 7 (b) shows that the surface coverage with cooler temperature is more obvious. It can be observed that the dark blue colour dominates the mapping of the surface and overshadows the yellow and

orange colours. The image of phase 2 was captured in the wet season in December 2019, explaining the cooler temperature on their surfaces. This study concludes that the potential for rock slope instability in phase 2 is higher than in phase 1. This is related to the study of Guerin et al. [10], which states that cooler temperature represents the loose rock section.

4. Conclusion

This study used a drone-based thermal sensor, which proved that a feasible solution is needed to achieve reliable data by providing the detection of rock slope criticality on large-scale inaccessible-hazardous sectors while protecting the safety of operators. The instability of rock slopes in terms of temperature in a tropical climate can be initiated by various factors, mainly through vegetation coverage and rainfall, and these factors are vital in the deterioration of rock slopes. Over time, the potential of rock slope instability increased with the increase of wetting and drying cycles. Identifying rock slopes that might be unstable in the future is a more complex task. Thus, early planning is needed to mitigate or minimise the hazard of rockfall before it occurs.

This study shows that the surface temperature affects the rock slope stability in a tropical climate, where cooler temperature is more prone to rock slope failure, as can be observed from the surface mapping from both phase 1 and 2. The probability of rock slope failure is high in the cooler temperature in phase 1 and 2. The rock slope instability and failure can be identified using surface temperature. Furthermore, the data from the remote sensing drone are essential for the temporal database in long-term rock slope surveillance and monitoring. This study agrees that the outputs should be discussed and further analysed by geologists. The result is expected to show surface temperature interactions from the perspective of thermal remote sensing images.

Acknowledgements

The authors would like to express their profound gratitude to the Faculty of Built Environment and Survey (FABU), Universiti Teknologi Malaysia (UTM), for all the support provided. The authors would also like to express their gratitude to PLUS Sdn. Bhd. Section N5 manager, Tn. Hj. Baharuddin bin Mat Taib and his staff, Mr. Amran bin Mokhtar and Mr. Radhi, for their data collection and technical support in this work, which is greatly appreciated. The authors would like to thank Geolatitude Technology Sdn. Bhd., Kulai, Johor, for providing drone

technical expertise during field activities. Finally, the authors would like to express their gratitude to PLUS Sdn. Bhd. and the Center of Excellence for the research partnership grant provided under UTM CR DTD VOT 4C585 and UTM IIIIG VOT 01M78.

References

- [1] Agliardi, F., Crosta, G., Zanchi, A., "Structural constraints on deep-seated slope deformation kinematics". *Eng. Geol.*, 59, 83-102, 2001.
- [2] Akinola, A. I., Wynn-Thompson, T. & Olgun, C. G. & Mostaghimi, S. & Eick, M. J., Fluvial "Erosion Rate of Cohesive Streambanks Is Directly Related to the Difference in Soil and Water Temperatures". *Journal of Environment Quality*. 48. 10.2134/jeq2018.10.0385, 2019.
- [3] Alejano, L., Gómez-Márquez, I. & Martínez-Alegría, R., "Analysis of a complex toppling-circular slope failure". *Engineering Geology - ENG GEOL*. 114. 93-104.10.1016/j.enggeo.2010.03.005,2010.
- [4] Al-Bared, M., Harahap, I., Marto, A., Mustaffa, Z., Ahmed, M., Alsubal, S.. Stability of cut slope and degradation of rock slope forming materials – a review. *Malaysian Construction Research Journal*. 6. 215-228, 2019.
- [5] Basahel, H. Mitri, H., "Application of rock mass classification systems to rock slope assessment: a case study " (J), 9 (6): 993-1009, 2007
- [6] Borges, R. G. Lima, A. C. D., Kowsmann, R. O. , "6 Areas susceptible to Landsliding on the Continental Slope", Editor: Renati Oscar Kowsmann, Geology and geomorphology, Campus, Pages 99-135, 2016.
- [7] Crosta, G., Agliardi, F., Frattini, P., Laris, S., "Key Issues in Rock Fall Modelling, Hazard and Risk Assessment for Rockfall Protection", 10.1007/978-3-319-09057-3_4.6, 2015.
- [8] Eisenbeiss, H., "UAV Photogrammetry, dissertation ETH No. 18515", Institute of Geodesy and Photogrammetry, ETH Zurich, Switzerland, Mitteilung 105, 2009.
- [9] Frodella, W., Gigli, G., Morelli, S., Lombardi, Luca & Casagli, N., "Landslide Mapping and Characterization through Infrared Thermography (IRT): Suggestions for

- a Methodological Approach from Some Case Studies". *Remote Sensing*. 9. 1281. 10.3390/rs9121281, 2017.
- [10] Guerin, A., Jaboyedoff, M., Collin, B., Derron, M.H., Stock, G., Matascai, B. Boesiger, M., Lefeuvre, C. & Podlaadchikov, Y., "*Detection of rock bridges by infrared thermal imaging and modelling*". Scientific Reports, 2019.
- [11] Gunzburge, Y., Soukatchoff, V. M. & Guglielmi, Y., "Influence of daily surface temperature fluctuations on rock slope stability: case study of Roches de Valbres Slope (France)". *International Journal of rock Mech and Mining Sciences*.42.3 331-349, 2005.
- [12] Harvey, M. C., Rowland, J. & Luketina, K. M., "Drone with Thermal Infrared Camera Provides High Resolution Georeferenced imagery of the Waikite Geothermal Area, New Zealand". *Journal of Volcanology and Geothermal Research*. 325. 61-69, 2016.
- [13] Hermanns, R. & Longva, O., "Rapid rock-slope failures. Landslide Types, Mechanisms and Modelling". 59-70, 2012.
- [14] Hoek, E. & Bray, J. W., "Rock Slope Engineering. Revised 3rd Edition", The Institution of Mining and Metallurgy, London, 341-351, 1981.
- [15] Huisman, M., Hack, H. R. G. K., Nieuwenhuis, J. D., "Observed rock mass degradation and resulting slope instability". *Proceeding of the EUROCK 2004 & 53rd geomechanics colloquy; rock engineering theory and practice, Salzburg, Austria, 7-9 October 2004*. Austrian Society for Geomechanics; Verlag Gluckauf VGE, Essen, 449-452, 2004.
- [16] Hungr, O., "Rock avalanche occurrence, process and modelling. In Landslides from Massive Rock Slope Failure". *Proceedings of the NATO Advanced Research Workshop on Massive Rock Slope Failure: New Models for Hazard Assessment, Celano, Italy, 16-21 June 2002*, ed. S. G. Evans, G. Scarascia Mugnozza, A. Strom and R. L. Hermanns. NATO Science Series IV, Earth and Environmental Sciences 49. Dordrecht, Netherlands: Springer, pp. 243-266, 2006.

- [17] Jansen, J., Codilean, A., Bishop, P., & Hoey, T., "Scale Dependence of Lithological Control on Topography: Bedrock Channel Geometry and Catchment Morphometry in Western Scotland". *The Journal of Geology*, 118(3), 223-246, 2010.
- [18] Kojan, E. & Hutchinson, J.N., "Mayunmarca rockslide and debris flow, Peru". In *Rockslides and Avalanches. 1. Natural Phenomena*, ed. B. Voight. Amsterdam: Elsevier Scientific Publishing Company, pp. 315–361, 1978.
- [19] Kovari, K. & Fritz, P., "Recent developments in the analysis and monitoring of rock slopes", *IVth International symposium on Landslides*, Toronto, 1984.
- [20] Luckman, B.H., "Processes, transport, deposition and landforms: rockfall". In: Shroder, J. (Editor in Chief), Marston, R.A., Stoffel, M. (Eds.), *Treatise on Geomorphology*. Academic Press, San Diego, CA, vol. 7, Mountain and Hillslope *Geomorphology*, pp. 174–182, 2013.
- [21] Małkowski, P., Kamiński P., & Skrzypkowski K., "Impact of heating carboniferous rocks on their mechanical parameters". *AGH Journal of Mining and Geoengineering*. Vol. 36, No 1, pp. 231–242, 2012.
- [22] Mattia, B., Bischetti, G. & Gentile, F., "Biotechnical characteristics of root systems of typical Mediterranean species. *Plant and Soil*, vol 278, no 1, pp. 23-32, 2005.
- [23] Noroozi, A. G. & Hajiannia, A., "The effect of vegetation on slope instability as predicted by the finite element method". 20. 13487-13496, 2015.
- [24] Norrish, N. I & Wyllie, D. C., "Landslides: Investigation and Mitigation". Chapter 15-Rock slope stability analysis; *Transportation Res. Board Spec. Report 247* 391–425, 1996.
- [25] Pantelidis, L., "Rock slope stability assesment through rock mass classification systems". *International journal of rock Mechanics and Mining sciences*, 46 (2), pp. 315-25, 2009.
- [26] Pinińska J, "The influence of elevated temperature on the mechanical properties of rocks". *Works of the Institute of Geotechnics and Hydrotechnics of the Wrocław University of Technology*, pp. 527–534, 2007.

- [27] Raghuvanshi, T. K., "Plane failure in Rock slopes A review on stability analysis techniques", *Journal of King Saud University - Science*, 2017, doi: <http://dx.doi.org/10.1016/j.jksus.2017.06.004>.
- [28] Robbins, B. A. , Stephens I.J. & Marcuson W.F., "Geotechnical Engineering", Editor(s): David Alderton, Scott A. Elias, *Encyclopedia of Geology (Second Edition)*, Academic Press, Pages 377-392, 2021.
- [29] Schuster, R. L. & Alford, D., "Usoi Landslide Dam and Lake Sarez, Pamir Mountains, Tajikistan". *Environmental and Engineering Geoscience*, 10, 151-168, 2004.
- [30] Shannon, H.R., Sigda, J.M., Van Dam, R.L., Hendrickx, J.M. & McLemore, V.T., "Thermal camera imaging of rock piles at the Questa Molybdenum Mine, Questa, New Mexico". In *Proceedings of the 22nd America Society of Mining and Reclamation Annual National Conference*, Breckenridge, CO, USA, 19–23 June; pp. 1015–1028, 2005.
- [31] Shibasaki, T., Matsuura, S. & Okamoto, T., "Experimental evidence for shallow, slow moving landslides activated by a decrease in ground temperature: Landslides affected by ground temperature". *Geophysical Research Letters*, 2016. 43.10.1002/2016GL069604.
- [32] Siad, L. & Megueddem, M., "Stability analyss of jointed rock slope". *Mech. Res. Commun.* 25. 661-700, 1998.
- [33] Spampinato, L., Calvari, S., Oppenheimer, C. & Boschi, E., "Volcano surveillance using infrared cameras. *Earth-Science Reviews*". 106. 63-91. 10.1016/j.earscirev.2011.01.003, 2011.
- [34] Tang, H., Yong, R., & Ez Eldin, M. A. M., "Stability analysis of stratified rock slopes with spatially variable strength parameters: the case of Qianjiangping landslide", *Bull. Eng. Geol. Environ.*, 2016. DOI 10.1007/s10064-016-0876-4.
- [35] Ulusay, R., "Harmonising engineering geology with rock engineering for assessing rock slopestability: A review of current practice". *Geotehnika*,4,pp. 1-16,2019.

- [36] United States Department of Agriculture Natural Resources Conservation Service. Part 631 Geology National Engineering Handbook, 2012. Retrieved from <https://directives.sc.egov.usda.gov/OpenNonWebContent.aspx?content=31848.wba>
- [37] Wyllie D.C. & Mah, C.W., "Rock slope engineering, civil and mining", 4th edn. Spon Press, Taylor & Francis Group, Great B, 2004.
- [38] Yang, Y. S.& Yeh, H. F., "Evaluate the Probability of Failure in Rainfall-Induced Landslides Using a Fuzzy Point Estimate Method". *Geofluids*. 1-15, 2019. 10.1155/2019/3587989.
- [39] Zhi-jun, W., Yang-Sheng Z., Yuan Z. & Chong W., "Research Status Quo and Prospection of Mechanical Characteris-tics of Rock under High Temperature and High Pressure". *Procedia Earth and Planetary Science No 1*, pp. 565–570, 2009.